IEEE Access
Multidisciplinary | Rapid Review | Open Access Journal

Received March 18, 2019, accepted April 2, 2019, date of publication April 22, 2019, date of current version May 3, 2019.

Digital Object Identifier 10.1109/ACCESS.2019.2912230

A Novel Shape Representation Method for Complex Trademark Image

BEN YE, ZHANCHUAN CAI, (Senior Member, IEEE), TING LAN, AND YOUQING XIAO
Faculty of Information Technology, Macau University of Science and Technology, Macau 999078, China

Corresponding author: Zhanchuan Cai (zccai@must.edu.mo)

This work was supported in part by the National Basic Research Program of China (973 Program) under Grant 2011CB302400, in part by the Science and Technology Development Fund of Macau under Grant 0012/2018/A1, Grant 0069/2018/A2, and Grant 048/2016/A2, in part by the National Natural Science Foundation of China under Grant 41371332, in part by the Open Project Program of State Key Laboratory of Virtual Reality Technology and Systems, Beihang University, under Grant VRLAB2019C02, in part by the Open Project Program of the State Key Lab of CAD&CG of Zhejiang University under Grant A1910, and in part by the Research and Development Fund of Beijing Institute of Technology, Zhuhai, under Grant XK-2018-04.

ABSTRACT Trademark orthogonal representation is an important research field in artificial intelligence technology and has extensive applications in trademark retrieval and recognition. However, the Gibbs phenomenon arises when complex trademark shapes are represented by using traditional methods, such as continuous orthogonal function and wavelet. In order to represent the complex trademark without Gibbs phenomenon, a novel method named hierarchical V-system (HV system) is proposed in this study, which is generated by V-system of multi-degree k ($k = 0, 1, 2, 3$). The hierarchical structure brings more detailed shape representation information. We show that the proposed method in this paper can represent the trademark shapes with fewer finite terms and obtain accurate representation result. This study also proposes the normalized descriptors of hierarchical V-system (HV descriptors). Furthermore, we demonstrate that the HV descriptors satisfy the invariance in rotation, translation, and scale transform. The experimental results show that the hierarchical V-system method can give reasonable descriptors for representing complex trademark without Gibbs phenomenon.

INDEX TERMS Complex trademark image, orthogonal representation, hierarchical V-system, descriptors.

I. INTRODUCTION

Trademarks as a kind of the important symbols symbolize the reputation and history of company. Retrieving and recognizing trademark image is always the important research trends of image processing and artificial intelligence. With the development of aesthetics, trademarks are endowed with more meanings, which makes trademark images more and more complex. These complex trademark images include not only triangles, circles, rectangles, and other basic geometric graphics, but also contains English letters, Chinese characters, Japanese characters, and other complex shapes (see Fig.1). In this paper, the complex trademark is defined as two (or more) separated trademark shapes sufficiently in an image. Some simple trademarks can be represented by continuous orthogonal functions or wavelets, but the representation of complex trademarks by using those methods causes Gibbs phenomenon. Therefore, a new orthogonal representation without Gibbs phenomenon can greatly help to retrieve and recognize complex trademark.

A huge amount of trademark images are transmitted via the internet. In this situation, there is a growing interest in trademark image retrieval [1]–[10] and trademark shape recognition [11]–[17]. How to represent two (or more) separated shapes sufficiently in a trademark image is an important issue [18]. Further, the representation of shape is the main content in complex trademark image retrieval because the shape is the most promising for the identification of entities in a trademark image [19], [20]. With the increasing number of images, the textual annotation of images becomes inefficient, and the content-based image retrieval (CBIR) has received growing interest in recent years [21]–[27]. In previous studies, the scale-invariant feature transform (SIFT) is used to describe the complex trademark shape in images [3], [9].

The associate editor coordinating the review of this manuscript and approving it for publication was Xiaogang Jin.

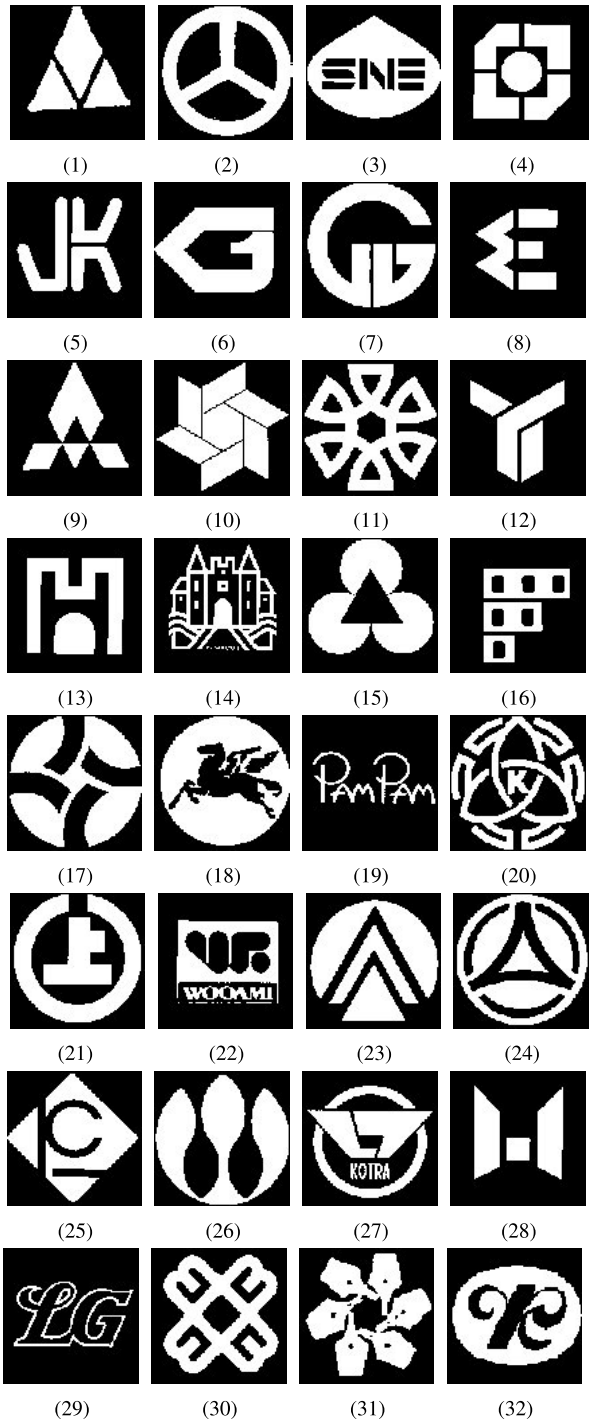

FIGURE 1. The dataset of binary complex trademark images (1-32) used in this paper are composed of multi-object shape. In the experiment section, the comparison of reconstruction efficiency is shown of the proposed method with Fourier series, Harr wavelet, and V^k-systems with degree$k$ ($k = 1, 2, 3$) is given.

However, the descriptors of SIFT is too complex for a complex trademark, which is detrimental to process a huge amount of trademark images. The ranking accuracy of current approaches using either hand-crafted or pre-trained deep convolution neural network (DCNN) features is inadequate for large-scale deployments [8]. Basically, a descriptor, which is effectual and suitable for the representation of complex trademarks, is one of the key parts to process large scale trademark dataset.

A variety of methods have been developed for the representation of complex trademark shape. The widely used methods are the Fourier series and the wavelet method, and it is well-known that orthogonal functions are the core of them. Until now, a vast number of approaches based on orthogonal functions have been presented. Indeed, not all complete orthogonal function systems are suitable for the analysis and synthesis of complex trademark image. Fourier system, Legendre system, and Chebyshev system are orthogonal function systems, but they cannot accurately represent the commonly complex trademark by finite terms, because the well-known Gibbs phenomenon may occur. Therefore, such schemes are not suitable for the representation of complex trademark. In fact, a method which can represent a group of complex trademarks precisely is needed in trademark representation.

A class of complete orthogonal system, called U-system, was proposed in 1984 [28]. U-system is composed by the piecewise polynomials of degree k ($k = 0, 1, 2, 3, \ldots$) on the interval $[0, 1]$ and has great advantages to deal with both continuous and discontinuous signals. Since U-system of degree 0 is the Walsh system, U-system of degree 1 is a slant transform that widely used in image processing, so U-system can be called as the generalization of the Walsh system. Based on U-system, a novel orthogonal function system named the V-system [29]–[32]. This novel and special orthogonal system is applied to many fields, e.g., triangulated domains [31], shape recognition [33], 3D model retrieval [34]. The V-system can be considered as the generalization of the Haar wavelet system because the Haar wavelet system is a special case of the V-system of degree 0.

To accurately represent the complex trademarks as few terms as possible, a new method named hierarchical V-system is proposed in this paper. More specifically, the hierarchical V-system comes from a hierarchical combination of V-system and inherits lots of properties from V-system. In particular, the hierarchical V-system scheme is an effective and powerful tool in the representation of the complex trademark by finite terms without Gibbs phenomenon. The representation performance of the proposed HV-system is tested in two scenarios, i.e., comparing the number of reconstruction term on same reconstruction precision, comparing the reconstruction precision on same number of reconstruction term.

Briefly speaking, our main contributions can be summarized as

- The hierarchical V-system (HV-system) is proposed, which is used for the task of representation complex trademark and achieves state-of-the-art results.
- The detailed formula of HV system and HV descriptors are shown in this paper, the construction flow and algorithm of HV system and HV descriptors are described in detail.

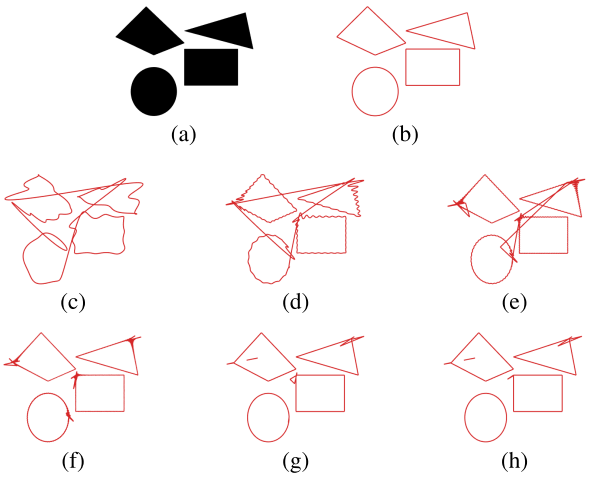

FIGURE 2. Diagram: Gibbs phenomenon in orthogonal representation of complex trademark. (a) Complex trademark image. (b) Complex trademark shape. (c) Fourier with 30 terms. (d) Fourier with 100 terms. (e) Fourier with 255 terms. (f) Fourier with 450 terms. (g) Daubechies-2(db2) wavelet with 1301 terms. (h) Daubechies-2(db2) wavelet with 1860 terms.

- The nature of HV descriptors which have invariance in rotation, translation, and scale transforms is expounded by proof and experiments.
- Extensive experiments are performed to show the efficiency of our proposed method on a variety of complex trademarks.

The rest of this paper is organized as follows. V-system and Gibbs phenomenon are reviewed in Section II. Section III describes the generation method of hierarchical V-system and hierarchical V-descriptors in detail. In Section IV, the performance of reconstruction and descriptors is revealed by experiments. Conclusions are given in Section V.

II. RELATED WORKS

A. GIBBS PHENOMENON

The Gibbs phenomenon, discovered by Wilbraham (1848) [35], [36] and named after Gibbs (1898,1899) [37], [38], describes the peculiar manner in which the Fourier series of a piecewise continuously differentiable periodic function behaves at a jump discontinuity. At jump discontinuities, the undershoot or overshoot is called the Gibbs phenomenon.

The Gibbs phenomenon is bound to happen when a discontinuous function is represented by continuous wavelet transform. An example is shown in Fig. 2, this example shows that the Gibbs phenomenon reflects the difficulty in representing a discontinuous shape by a finite series of orthogonal continuous function and continuous waves.

B. V-SYSTEM

The definition, construction, and mathematical analysis of V-system are given [29], and the detailed generation method of V-system function of degree k ($k = 1, 2, 3$) is provided in Appendix. Here the V-system of degree k are introduced briefly.

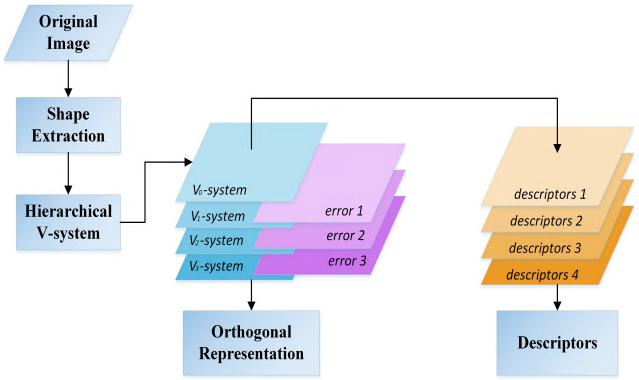

FIGURE 3. Structure of hierarchical V-system.

The V-system of degree k is ordered by classes and groups. The first group contains only one class consisting of the first $k+1$ functions which are the Legendre polynomials on [0, 1]. It is denoted as

$$\{V_{k,1}^1(x), V_{k,1}^2(x), \ldots, V_{k,1}^{k+1}(x)\} \tag{1}$$

The second group also contains only one class consisting of the second $k+1$ functions which are the k^{th}-order generators. It is denoted as

$$\{V_{k,2}^1(x), V_{k,2}^2(x), \ldots, V_{k,2}^{k+1}(x)\}. \tag{2}$$

From the beginning of the third group of the V-system of degree k, the m^{th} group consists of $k+1$ classes, and each class includes 2^{m-2} functions. We denote $V_{k,m}^{i,j}(x)$ as the j^{th} function in the i^{th} class of the m^{th} group in the V-system of degree k, where $k = 0, 1, 2, \ldots; m = 3, 4, \ldots$ and $j = 1, 2, \ldots, 2^{m-2}$. From the beginning of the third group of the V-system, each group consists of $k+1$ classes, and each class has 2^{m-2} functions. The V-system of degree $k = 0$ is the Haar function system which is one of the most important and widely known wavelets.

III. HIERARCHICAL V-SYSTEM

A. MOTIVATION

In complex trademarks, two (or more) sufficiently separated shape in a trademark image include continuous and discontinuous graphics. Using the Fourier method to reconstruct complex trademark, the Gibbs phenomenon appears. In order to accurately represent the complex trademark with finite terms and to explore the spectral properties of complex trademark, the hierarchical V-system scheme is proposed. The series expansion of hierarchical V-system has good square approximation and uniform approximation, which uses the finite terms of series to realize the accurate expression of complex trademark. For the representation of a complex trademark under the same precision, the terms of series with the hierarchical V-system method are fewer than that with the V-system method.

B. ALGORITHM

In this section, the methodology of hierarchical V-system is described in detail. Fig. 3 and Pseudo Code 1 give the structure and code of hierarchical V-system, respectively. The processing of trademark shape extraction is stated in Section IV-A. For convenience, supposing that the interval [0, 1] is equally divided into n sub-intervals, and t varies in the interval [0, 1]. We use multiple approximation functions $f_0, r_1, \cdots, r_k$, and the representation function of a complex trademark is denoted by $F(t)$, i.e.

$$F(t) = g_i(t), \tag{3}$$

where $t \in [\frac{i}{n}, \frac{i+1}{n}]$, $i = 0, 1, \cdots, n$.

Then, the shape of a given complex trademark is represented as a parameter form, and such form can be defined as

$$\begin{cases} x(t) = F_x(t), \\ y(t) = F_y(t). \end{cases} \tag{4}$$

The V-system of degree 0 is performed on a complex trademark, and the function f_0 can be obtained. The function f_0 is the initial function in the hierarchical V-system of degree 0, and it can be expressed as

$$f_0 = \sum_{i=1}^{N_1} a_i^{(0)} V_i^{(0)}, \tag{5}$$

where $V_i^{(0)}$ means the V-system of degree 0, the general terms of $V_i^{(0)}$ can be found in Appendix. Given a threshold ε, and then the value of N_1 can be calculated. Moreover, an error can be obtained, i.e.,

$$f_1 = F(t) - f_0. \tag{6}$$

Meanwhile, the norm of function f_1 denoted as $||f_1||$ can be computed. Comparing ε with $||f_1||$, when $\varepsilon \geqslant ||f_1||$, N_1 is obtained, and then function f_2 can be computed. It is the approximated function in the hierarchical V-system of degree 2, and f_2 is

$$f_2 = f_1 - \sum_{i=1}^{N_2} a_i^{(1)} V_i^{(1)}, \tag{7}$$

where $V_i^{(1)}$ means the V-system of degree 1, the general formula of $V_i^{(1)}$ can be found in Appendix. Moreover, the norm of function f_2 denoted as $||f_2||$ can be computed. Comparing ε with $||f_2||$, when $\varepsilon \geqslant ||f_2||$, N_2 is obtained, and then the function f_3 can be computed.

In the same way, the function f_k can be obtained

$$f_k = f_{k-1} - \sum_{i=1}^{N_k} a_i^{(k-1)} V_i^{(k-1)}, \tag{8}$$

where $V_i^{(k)}$ means the V-system of degree k, the general terms of $V_i^{(k)}$ can be found in Appendix. Then, the norm of function f_k denoted as $||f_k||$ can be computed. Comparing ε with f_k, when $||f_k||$ is reached the given precision, the hierarchical iteration should be stopped. Ultimately, the number of reconstruction terms is $N_1 + N_2 + \cdots + N_k$, and the approximation function is $\breve{f} = f_0 + f_1 + f_2 \ldots + f_k$.

By orthogonality, we have

$$a_i^{(k)} = \int_0^1 \begin{pmatrix} x(t) \\ y(t) \end{pmatrix} V_j^{(k)}(t)dt, \quad j = 0, 1, 2, \cdots, \quad n-1; \ k = 0, 1, 2, \cdots h, \tag{9}$$

where $V_j^{(k)}(t)$ means the V-system of degree k. And we have

$$P(t) = \begin{pmatrix} x(t) \\ y(t) \end{pmatrix} = \sum_{k=0}^{h} \sum_{\iota=0}^{N_k} a_\iota^{(k)} V_\iota^{(k)}(t). \tag{10}$$

The shape of a given complex trademark can be reconstructed. i.e., for a given complex trademark $F(t)$, we can use $P(t)$ pairs of segmentation for representing the n-segment straight-line group under finite precision expression.

C. DESCRIPTORS OF HIERARCHICAL V-SYSTEM (HV DESCRIPTORS)

The feature with the invariance in rotation, translation, and scale transforms is very important for complex trademark retrieval. This section discusses the rotation, translation, and scale transforms of hierarchical V-system, and such features are called the descriptors of hierarchical V-system. Given a complex trademark with 2^n pieces in 2D space, the horizontal $x(t)$ and vertical $y(t)$ coordinates of the contour points can be expressed as

$$P(t) = x(t) + iy(t), \tag{11}$$

where $i = \sqrt{-1}$.

The interval [0,1] is partitioned into 2^n subintervals $I_j = [\frac{j}{2^n}, \frac{j+1}{2^n}]$, where $j = 0, 1, \cdots, 2^n - 1$, and then $x(t)$ and $y(t)$ are mapped on the subintervals,

$$\begin{cases} x(t) = x_j(t), \\ y(t) = y_j(t), \end{cases} \quad \text{if } t \in I_j, \quad j = 0, 1, 2, \cdots, 2^n - 1, \tag{12}$$

where $x_j(t)$ and $y_j(t)$ are the polynomials of degree k on the interval I_j. By the reproducibility of the V-series and the $k+1$ coefficients of the polynomial of degree k, we have

$$\begin{aligned} P(t) &= x(t) + iy(t) \\ &= \sum_{k=0}^{h} \sum_{j=0}^{N_h} a_x^{(k),(j)} V_j^{(k)}(t) + i \sum_{k=0}^{h} \sum_{j=0}^{N_k} a_x^{(k),(j)} V_j^{(h)}(t), \end{aligned} \tag{13}$$

where

$$\begin{cases} a_x^{(k),(j)} = \int_0^1 x(t) V_j^{(k)}(t)dt, \\ a_y^{(k),(j)} = \int_0^1 y(t) V_j^{(k)}(t)dt, \end{cases} \quad j = 0, 1, 2, \ldots, 2^n - 1,$$

Pseudo Code 1 Hierarchical V-System Algorithm

Input: Function of a complex trademark $F(t)$;
  Given a threshold ε.
Output: Reconstruction function of complex trademark
trademark
Let $F(t)$ convert into a parameter form
compute $\breve{f}$ with **Hierarchical V-system** ($F(t)$)
case 1**:**
  The function of the first curve
case 2**:**
  The function of the second curve
  ⋮
case k**:**
  The function of the k**-th curve**
Obtain reconstruction function:
$\breve{f} = f_0 + f_1 + f_2 + \ldots + f_k$
Procedure Hierachical V-system $F(t)$
for $k \leqslant \infty$ **do**
  $f_0 = \sum_{i=1}^{N_1} a_i^{(0)} V_i^{(0)}$
  $a_i^{(k)} = \int_0^1 \begin{pmatrix} x(t) \\ y(t) \end{pmatrix} V_i^{(k)}(t)dt$
  $i = 0, 1, 2, 3, \ldots, k$
  $f_k =$**V-system Transform**(a_i, k, ε)
  $f_k = F(t) - f_{k-1}$
  if then norm: $||f_k|| \approx 0$
    Stop loop
  end if
end for
end Procedure
Hierarchical V-system (a_i, k, ε)
for $j = 1$ **to** N_k **do**
  $f_k = f_{k-1} - \sum_{j=1}^{N_k} a_j^{(k-1)} V_j^{(k-1)}, k \geqslant 1$
  if norm: $||f_k|| \leqslant \varepsilon$ **then**
    return f_k
  end if
end for
end Function

Note $a^{(k)}(j) = a^{(k)j}_{\ x} + i a^{(k)j}_{\ y}$, where $a^{(k)}(j)$ is called as the j-th descriptors of $P(t)$, and its form is

$$a^{(k)}(j) = \int_0^1 x(t) V_j^{(k)}(t)dt + i \int_0^1 y(t) V_j^{(h)}(t)dt = \int_0^1 P(t) V_j^{(k)}(t)dt, \tag{14}$$

and then we can obtain

$$P(t) = \sum_{k=0}^{h} \sum_{j=0}^{N_k} a^{(k)}(j) V_j^{(k)}(t). \tag{15}$$

Furthermore, we define the *energy* of the complex trademark $P(t)$ as

$$E = \Big(\sum_{j=0}^{N_h} ||a^{(k)}(j)|| \Big)^{\frac{1}{2}}. \tag{16}$$

Since the orthogonal transformation preserves the length, the above energy E is invariant in rotation for the same complex trademark. Using this feature, we can conduct recognition and classification on the complex trademark databases. In the retrieval of complex trademarks, the definition of the normalized descriptors of hierarchical V-system is important. In order to make the descriptors that can satisfy the invariance in rotation, translation, and scale transforms, the normalized descriptors are defined as following:

Let

$$D(j) = \frac{||a^{(k)}(j)||}{||a^{(k)}(max)||}, \quad j = 1, 2, \cdots, \tag{17}$$

where $D(j)$ is called the j-th unified descriptors of $P(t)$. Especially, when $j = 0$, we call $D(0)$ as "DC" term.

Theorem: (1) For $j = 0, 1, 2, \cdots$, via a shifting transformation z_0, a scaling transformation β, and a rotation transformation ϑ, the descriptors $a^k(j)$ of $P(t)$ can be transformed into

$$\bar{a}^{(k)}(j) = \beta e^{i\vartheta}[a^{(k)}(j) + z_0\delta(j)], \tag{18}$$

where

$$\delta(j) = \begin{cases} 0, & j \neq 0, \\ 1, & j = 0. \end{cases} \tag{19}$$

(2) The unified descriptors $D(j), j = 1, 2, \cdots$ are invariant under shifting, scaling, and rotation transformations.

Proof: (1) Let the shifting displacement be z_0, the scaling be β, and the rotation angle be ϑ, and then the new shape is the form as $P_1(t) = \beta e^{b\vartheta}(P(t) + z_0)$, and its descriptors are

$$\begin{aligned} \bar{a}^{(k)}(j) &= \int_0^1 \beta e^{i\vartheta}(P(t) + z_0) V_j^{(k)}(t)dt \\ &= \beta e^{i\vartheta}\Big(\int_0^1 P(t) V_j^{(k)}(t)dt + \int_0^1 z_0 V_j^{(k)}(t)dt\Big) \\ &= \beta e^{i\vartheta}[a^{(k)}(j) + z_0\delta(j)], \end{aligned} \tag{20}$$

where $\int_0^1 V_j^{(k)}(t)dt = \delta(j) = \begin{cases} 0, & j \neq 0, \\ 1, & j = 0. \end{cases}$

(2) For $j = 1, 2, \cdots$, it follows from (1) that $\bar{a}^{(k)}(j) = \beta e^{i\vartheta} a^{(k)}(j)$, and

$$\bar{D}(j) = \frac{||\bar{a}^{(k)}(j)||}{||max(\bar{a}^{(k)})||} = \frac{||a^{(k)}(j)||}{||max(a^{(k)})||} = D(j) \tag{21}$$

■

Let $D_A(j)$ and $D_B(j)$) be the unified descriptors of two trademarks A and B expressed by piecewise polynomials, respectively. There exists a number N such that A and B can be exactly expressed by the N terms of the V-system. Therefore, we define the distance of the trademark A and B as follows:

$$\Upsilon = \sqrt{\sum_{j=1}^{N} ||D_A(j) - D_B(j)||^2}. \tag{22}$$

By means of the concept of the distance of two trademarks, we can approximately measure how similar the trademark

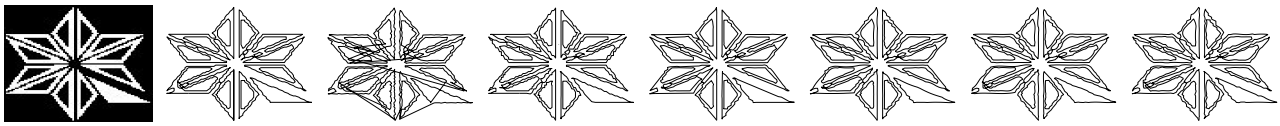

FIGURE 4. Representation of Hexagon with identical construction precision and different number of construction term. (a) Complex trademark image. (b) Complex trademark shape. (c) Fourier reconstruction with 765 terms. (d) Haar wavelet reconstruction with 558 terms. (e) V-system of degree 1 reconstruction with 383 terms. (f) V-system of degree 2 reconstruction with 423 terms. (g) V-system of degree 3 reconstruction with 448 terms. (h) Hierarchical V-system reconstruction with 311 terms.

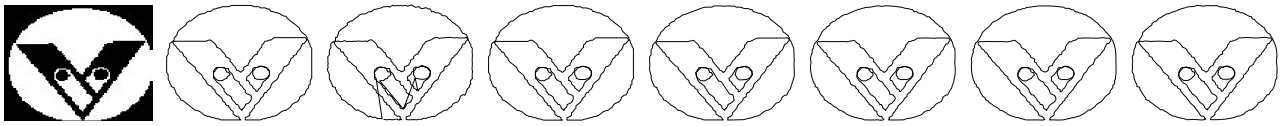

FIGURE 5. Representation of Mark with identical construction precision and different number of construction term. (a) Complex trademark image. (b) Complex trademark shape. (c) Fourier reconstruction with 345 terms. (d) Haar wavelet reconstruction with 449 terms. (e) V-system of degree 1 reconstruction with 209 terms. (f) V-system of degree 2 reconstruction with 209 terms. (g) V-system of degree 3 reconstruction with 199 terms. (h) Hierarchical V-system reconstruction with 126 terms.

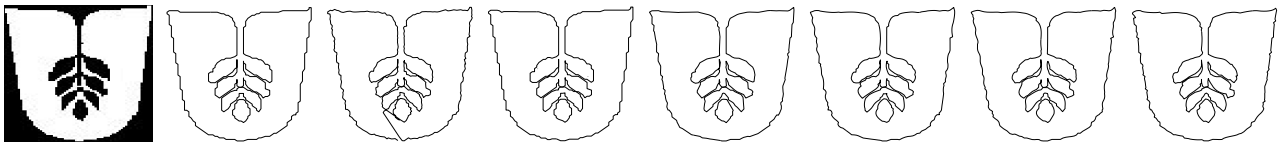

FIGURE 6. Representation of Leaf with identical construction precision and different number of construction term. (a) Complex trademark image. (b) Complex trademark shape. (c) Fourier reconstruction with 270 terms. (d) Haar wavelet reconstruction with 354 terms. (e) V-system of degree reconstruction with 164 terms. (f) V-system of degree 2 reconstruction with 164 terms. (g) V-system of degree 3 reconstruction with 169 terms. (h) Hierarchical V-system reconstruction with 99 terms.

are, and we can also recognize the complex trademark shape with the property of shifting, scaling, and rotation invariance. The bigger distance Υ is, the bigger the difference of two trademarks is. $\Upsilon = 0$ means the shapes of the two models are same.

IV. EXPERIMENTS AND ANALYSIS

In this section, the performance of the hierarchical V-system algorithm on orthogonal representation is tested. In the experiments, when the error of the reconstructed trademark is less than e, the complex trademark can be considered as accurate reconstruction. In the following, the orthogonal representation of the hierarchical V-system for representing complex trademarks is discussed first.

A. SHAPE EXTRACTION

Shape representation means obtaining a set of features for characterizing the shape, and such features can be used to reconstruct shape. The following steps show the processed of shape extraction step.

1. A true color image or a grayscale image is converted into the binary image.

An image includes target objects and background noise. In order to extract target objects directly from multiple value digital image, a global threshold T is set. Thresholding creates binary images from grey-level ones by turning all pixels below threshold T to zero and all pixels about that threshold to one. When the image $I'(x, y)$ is a thresholded image of the grayscale image $I(x, y)$ under the global threshold T, it has the form:

$$I'(x,y) = \begin{cases} 1, & \text{if } I(x,y) \geqslant T, \\ 0, & \text{otherwise}, \end{cases} \tag{23}$$

where (x, y) represents the pixel values.

2. Gaussian blur

In image processing, a Gaussian blur is the result of blurring an image that uses a Gaussian function for calculating the transformation to apply to each pixel in the image. The equation of a Gaussian function in two dimensions is

$$G(x,y) = \frac{1}{2\pi\sigma^2} e^{-\frac{x^2+y^2}{2\sigma^2}},$$

where x is the distance from the origin in the horizontal axis, y is the distance from the origin in the vertical axis, and σ is the standard deviation of the Gaussian distribution.

3. Contour extraction

When the edge image is obtained by the Canny edge detector, the pixel values of the edge image can be represented as $f(x, y)$, each line-scan terminates in the following two cases:

(1) $f(x, y-1) = 0, f(x, y) = 1$ wherein $f(x, y)$ is the starting point of the outer boundary;

(2) $f(x, y-1) \geqslant 1, f(x, y+1) = 0$, wherein $f(x, y)$ is the starting point of the hole boundary. Then, we should start from the starting point and mark the pixels on the edge. Here, a unique identifier called *NBD* is assigned to the new

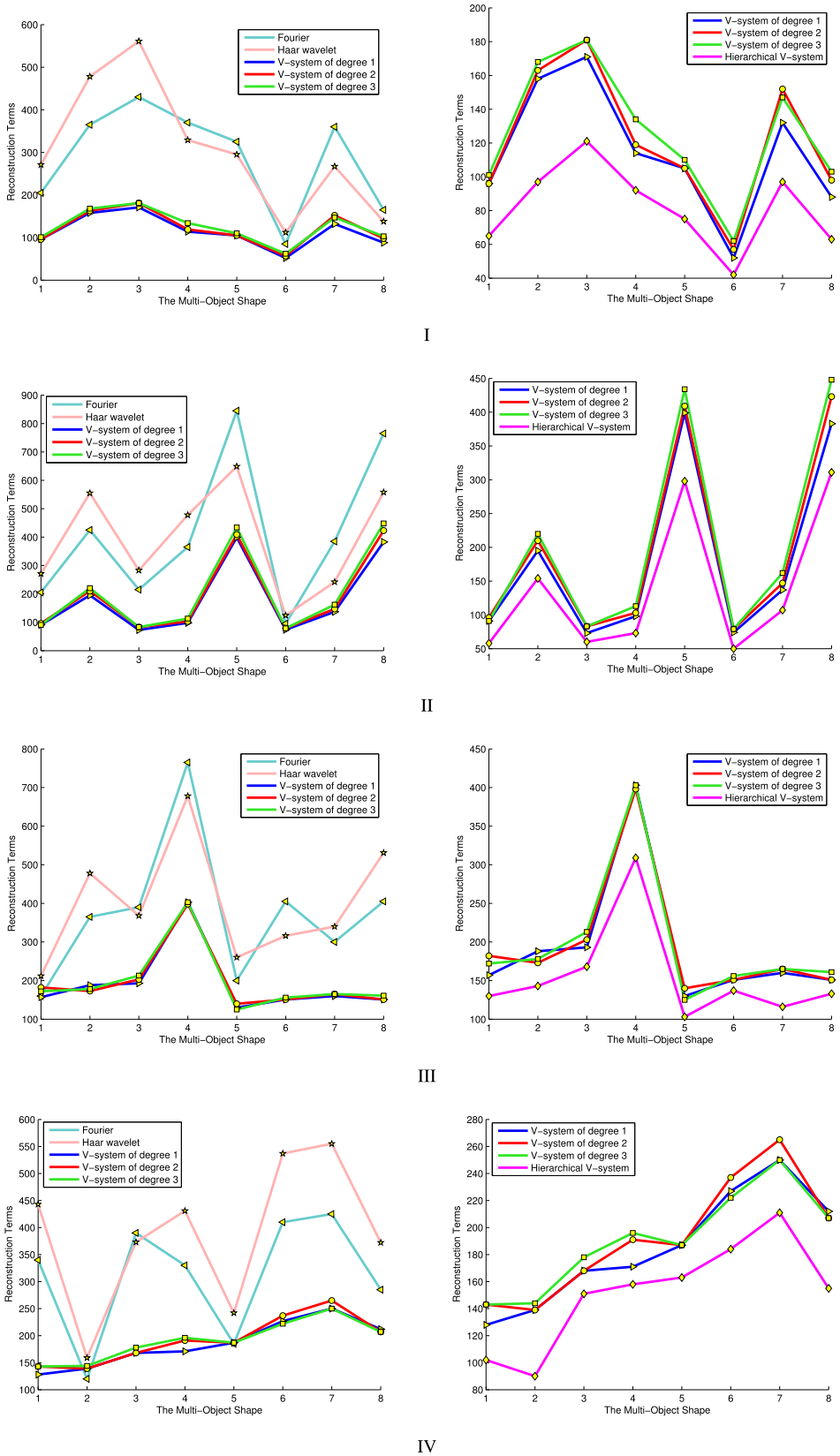

FIGURE 7. Reconstruction terms by using different methods (Fourier, Harr wavelet, V-system of degree k ($k = 1, 2, 3$)). I The construction result and relationship of complex trademarks 1-8. II The construction result and relationship of complex trademarks 9-16. III The construction result and relationship of complex trademarks 17-24. IV The construction result and relationship of complex trademarks 25-32.

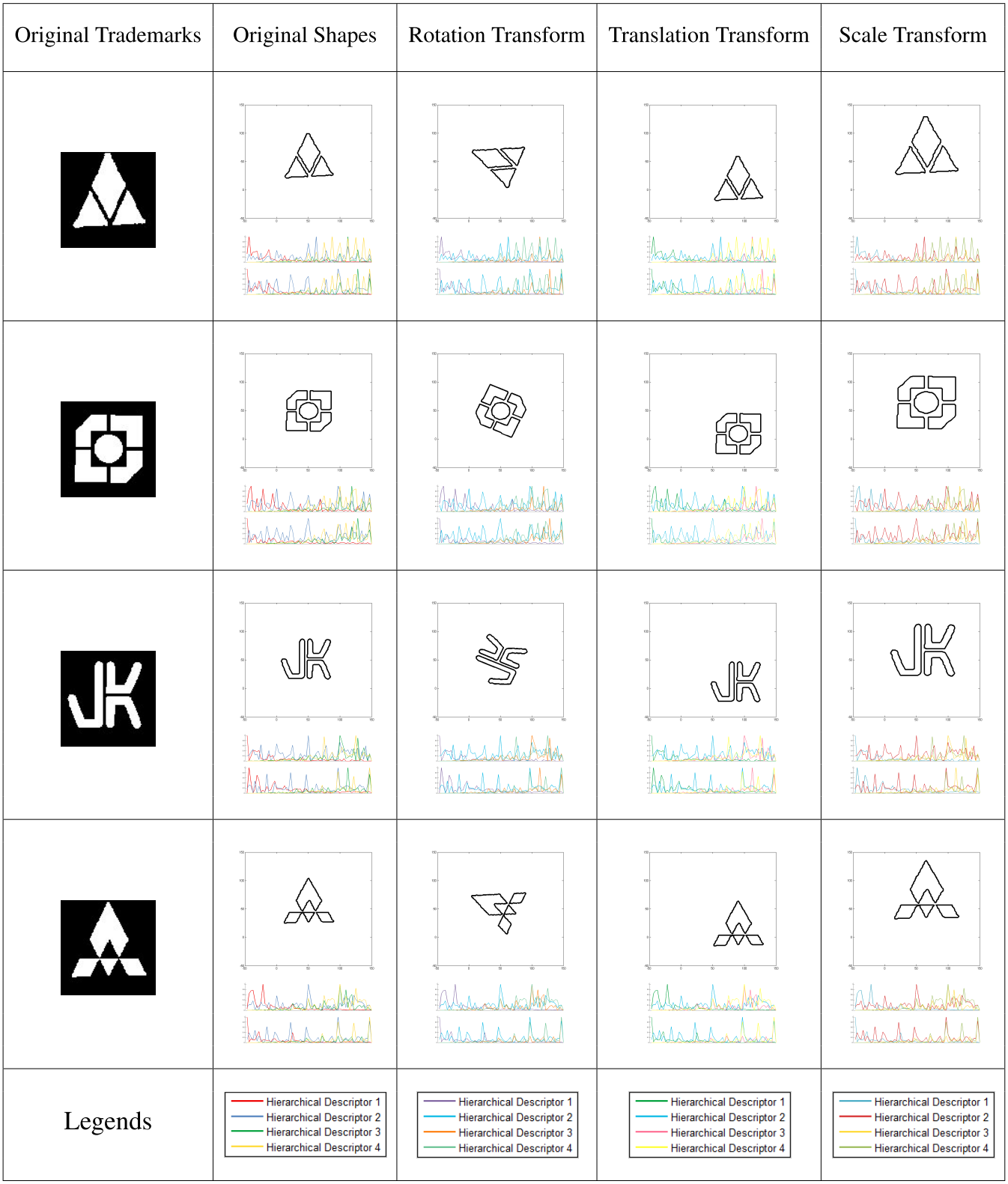

FIGURE 8. The invariance experiments of hierarchical V-system descriptors. Four examples with regular complex trademark and irregular complex trademark, the results contains the original, rotate, translation, and scale transform shape and their energy frequency descriptors of x and y.

discovered edge. The initial NBD is equal to 1, when a new boundary is found, NBD pluses one. And, $f(x, y)$ is set to $-NBD$ when $f(x, y) = 1$ and $f(x, y + 1) = 0$. According to the area and perimeter of the target trademark, an area threshold T' is set. When the area of an trademark is less than the threshold T', it is removed. Otherwise, it is reserved.

4. According to the perimeter and the number of points, the length of each contour segment can be calculated. Then, according to the length of each contour segment, linear interpolation can be done in the contour, and the most qualified points are obtained. In addition, the correction is used for the points. Because of the accuracy of floating-point precision of linear interpolation, it is possible that the number of points is not enough. Therefore, the points should be completed that less than the number of segment points. And the coordinates of the complete points are chosen directly from the coordinates of the last point.

B. RECONSTRUCTION AND DESCRIPTORS

This section provides complex trademark images to illustrate the results of different complex trademarks by using the Fourier method, the Haar wavelet method, the V-system method, and the hierarchical V-system method, as shown in Fig. 4, 5 and 6. In the experiments, the reconstruction of complex trademark with continuous wavelets (such as db2 wavelet) causes the Gibbs phenomenon. Therefore, a non-continuous wavelet named Haar wavelet is selected.

The comparison results among the reconstruction terms of the Fourier method, the Haar wavelet method, the V-system method, and the hierarchical V-system method results are shown in Fig.7. The number of reconstruction terms with the Fourier method, the Haar wavelet method, and the V-system method (degree 1, 2, 3) for different images are shown in Fig.7.I (right), Fig.7.II (right), Fig.7.III (right), and Fig.7.IV (right), respectively. It can be found that the number of reconstruction terms with the V-system method (degree 1, 2, 3) are fewer than that with the Fourier method and the Haar wavelet method. Under the same conditions, the number of reconstruction terms with the V-system method (degree 1, 2, 3) and the hierarchical V-system method are compared, as shown in Fig.7.I (left), Fig.7.II(left), Fig.7.III(left) and Fig.7.IV(left). We can find that the reconstruction terms of the hierarchical V-system method are also fewer than that with V-system method (degree 1, 2, 3) when the complex trademark are same. In addition, two standard shape databases are selected in the experiments. The first is the MPEG.7 shape database which consists of 1400 images classified into 70 classes [39]. The shapes of the images in this database are derived from natural objects, man-made objects, objects extracted from cartoons, and manually-drawn objects under various rigid and non-rigid deformations. The importance of this database is due to the fact that it is the only set used to objectively evaluate the performance of various shape descriptors. And another selected is the Kimia's database which contains 99 images with 9 categories [40]. There are 11 images for each category and most of the images are partially occluded. Ultimately, 32 images are randomly selected from these two databases, as shown in Fig.7.

In Fig.7, the horizontal axis represents different complex trademark images, and the vertical axis represents the number of reconstruction terms. The number ''1'' on the horizontal axis in Fig.7.I represents the complex trademark image in Fig.1.(1); The number ''2'' on the horizontal axis in Fig.7.I represents the complex trademark t image in Fig.1.(2); The rest can be done with the same manner until the number ''8'' on the horizontal axis in Fig.7.I represents the complex trademark image in Fig.1.(8). Fig.7.II and Fig.1.(9-16), Fig.7.III and Fig.1.(17-24), Fig.7.IV and Fig.1.(25-32) also have the same correspondence relationship as Fig.7.I and Fig.1.(1-8).

As a key point of image retrieval, the descriptors should have the features with the invariance in rotation, translation, and scale transform. The Fig.1.(1),Fig.1.(4), Fig.1.(5), and Fig.1.(7) are chosen as the research objects on hierarchical V-system descriptors invariance experiment, because they includes approximate shape with axisymmetric, centrosymmetric, letter, and circle. In Fig. 8, the first column shows the selected original images, and other column contains shape in axis and descriptors in real(x) frequency and imaginary(y) frequency. The last row shows the descriptors legend of each column. Obviously, the HV descriptors are invariable in each hierarchy for a same original complex trademark. And each layer of hierarchical V-descriptors are invariable for rotation, translation, and transform. The hierarchical descriptors have four layer information to describe the shape. Therefore, the hierarchical V-descriptors are more accurate than other layer descriptors for representing complex trademark.

V. CONCLUSION

In complex trademark retrieval, the representation of complex trademark is very important. Since complex trademarks contain the continuous graphics and the discontinuous graphics, the representation of complex trademark with traditional methods (such as the Fourier series and continuous wavelet transform) causes Gibbs phenomenon, i.e., the Fourier series and continuous wavelet transform cannot exactly represent the commonly complex trademark by using finite terms because they have strong continuity. Therefore, they are not suitable for the representation of complex trademarks. And using V-system, the accurate representation of complex trademarks can be achieved by finite terms without Gibbs phenomena. In order to represent complex trademark with the number of finite terms as few as possible under the same accurate representation. This study proposes hierarchical V-system, which is a hierarchical combination of V-system and inherits lots of properties from V-system. Moreover, this study defines the descriptors of hierarchical V-system and their normalization and gives the corresponding derivation process. And the invariance in rotation, translation, and scale transforms of the normalized hierarchical V-system descriptors are theoretically proved.

This paper also did several experiments for verifying the effectiveness of the proposed method. The experimental results show that the orthogonal representation of complex trademarks with hierarchical V-system has no Gibbs phenomenon by finite terms, and the number of reconstruc-

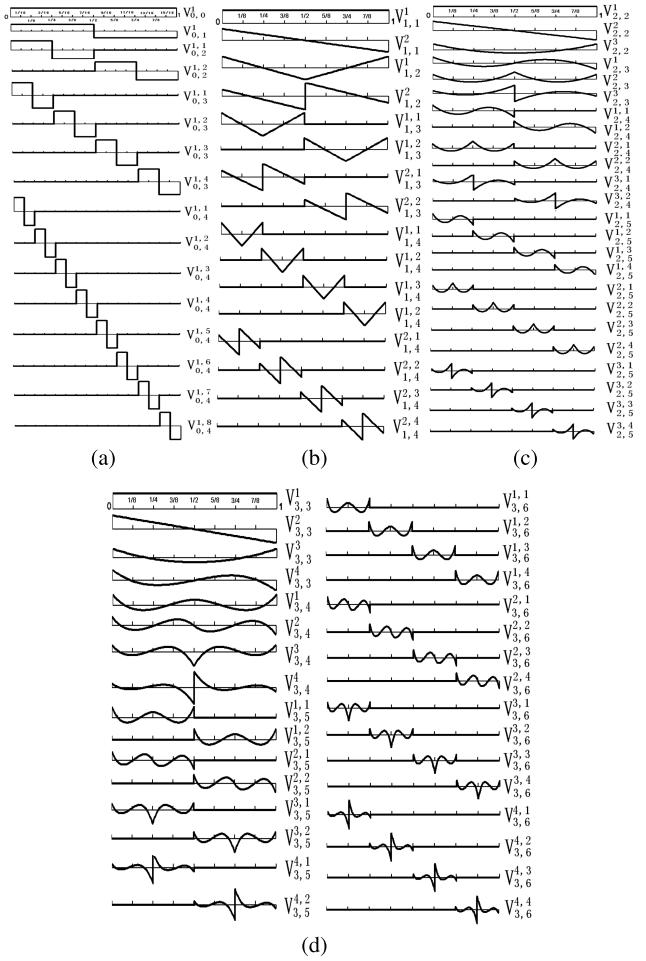

FIGURE 9. Some functions of V-system of degree $k = 0, 1, 2, 3$. (a) The first 16 basis functions with $k = 0$. (b) The first 16 basis functions with $k = 1$; (c) The first 24 basis functions with $k = 2$. (d) The first 32 basis functions with $k = 3$.

tion terms using hierarchical V-system for representing the a complex trademark are fewer than that using V-system, Fourier transform, and Haar system under the same accurate representation. The normalized descriptors of hierarchical V-system satisfies the invariance in rotation, translation, and scale transforms, which provides a good method for complex trademark retrieval. In future, we will analyze complex trademark retrieval based on hierarchical V-system descriptors.

ACKNOWLEDGEMENT

The authors wou ld like to thank Prof. Dongxu Qi for providing helpful and useful suggestions.

APPENDIX: GENERAL TERMS OF THE V-SYSTEM

Let the functions $V_{k,1}^1(x), V_{k,1}^2(x), \cdots, V_{k,1}^{k+1}(x)$ be the first $(k+1)$ Legendre polynomials on the interval $[0, 1]$, the function generator is defined as $F(x) = \{V_{k,2}^i(x)\}_1^{k+1}$, any two functions in the set $F(x)$ are orthogonal each other, and any one function in $F(x)$ is orthogonal with $V_{k,1}^1(x), V_{k,1}^2(x), \cdots, V_{k,1}^{k+1}(x)$. Fig. 9 shows the basis functions of the V-system of degree k, $k = 0, 1, 2, 3$.

The V-system of degree k is defined as follows:

$$V_{k,n}^{i,j}(x) = \begin{cases} \sqrt{2^{n-2}} V_{k,2}^i[2^{n-2}(x - \frac{j-1}{2^{n-2}})], & x \in (\frac{j-1}{2^{n-2}}, \frac{j}{2^{n-2}}), \\ 0, & \text{others}, \end{cases}$$

where $i = 1, 2, \cdots, k+1$, $j = 1, 2, \cdots, 2^{n-2}$, $n = 3, 4, 5, \cdots$.

In particular, when $k = 0$, the V-system is

$$V_{0,1}^1(x) = 1, x \in [0, 1],$$
$$V_{0,2}^1(x) = \begin{cases} 1, & x \in [0, \frac{1}{2}), \\ -1, & x \in [\frac{1}{2}, 1). \end{cases}$$

The general terms of the V-system of degree 0 are given by

$$V_{0,n}^{1,j}(x) = \begin{cases} \sqrt{2^{n-2}} V_{0,2}^1[2^{n-2}(x - \frac{j-1}{2^{n-2}})], & x \in (\frac{j-1}{2^{n-2}}, \frac{j}{2^{n-2}}), \\ 0, & \text{others}, \end{cases}$$

where $j = 1, 2, \cdots, 2^{n-2}$, and $n = 3, 4, \cdots$. Obviously, the V-system of degree 0 is the Haar system.

For $k = 1$, the V-system is

$$V_{1,1}^1(x) = 1, x \in [0, 1],$$
$$V_{1,1}^2(x) = \sqrt{3}(1 - 2x), \ x \in [0, 1],$$
$$V_{1,2}^1(x) = \begin{cases} \sqrt{3}(1 - 4x), & x \in [0, \frac{1}{2}), \\ \sqrt{3}(4x - 1), & x \in [\frac{1}{2}, 1), \end{cases}$$
$$V_{1,2}^2(x) = \begin{cases} 1 - 6x, & x \in [0, \frac{1}{2}), \\ 5 - 6x, & x \in [\frac{1}{2}, 1). \end{cases}$$

The general terms of the V-system of degree 1 are given by

$$V_{1,n}^{1,j}(x) = \begin{cases} \sqrt{2^{n-2}} V_{1,2}^1[2^{n-2}(x - \frac{j-1}{2^{n-2}})], & x \in (\frac{j-1}{2^{n-2}}, \frac{j}{2^{n-2}}), \\ 0, & \text{others}. \end{cases}$$
$$V_{1,n}^{2,j}(x) = \begin{cases} \sqrt{2^{n-2}} V_{1,2}^2[2^{n-2}(x - \frac{j-1}{2^{n-2}})], & x \in (\frac{j-1}{2^{n-2}}, \frac{j}{2^{n-2}}), \\ 0, & \text{others}. \end{cases}$$

where $j = 1, 2, \cdots, 2^{n-2}$, and $n = 3, 4, \cdots$.

For $k = 2$, the V-system is

$$V_{2,1}^1(x) = 1, \ x \in [0, 1],$$
$$V_{2,1}^2(x) = \sqrt{3}(1 - 2x), \ x \in [0, 1],$$
$$V_{2,1}^3(x) = \sqrt{5}(6x^2 - 6x + 1), \ x \in [0, 1],$$

$$V_{2,2}^1(x) = \begin{cases} \sqrt{5}(16x^2-10x+1), & x \in [0, \frac{1}{2}), \\ \sqrt{5}[-16(1-x)^2+10(1-x)-1], & x \in [\frac{1}{2}, 1), \end{cases}$$

$$V_{2,2}^2(x) = \begin{cases} \sqrt{3}(30x^2 - 14x + 1), & x \in [0, \frac{1}{2}), \\ \sqrt{3}[30(1-x)^2 - 14(1-x) + 1], & x \in [\frac{1}{2}, 1), \end{cases}$$

$$V_{2,2}^3(x) = \begin{cases} 40x^2 - 16x + 1, & x \in [0, \frac{1}{2}), \\ -40(1-x)^2 + 16(1-x) - 1, & x \in [\frac{1}{2}, 1). \end{cases}$$

The general terms of the V-system of degree 2 are given by

$$V_{2,n}^{1,j}(x) = \begin{cases} \sqrt{2^{n-2}} V_{2,2}^1[2^{n-2}(x - \frac{j-1}{2^{n-2}})], & x \in (\frac{j-1}{2^{n-2}}, \frac{j}{2^{n-2}}), \\ 0, & \text{others}, \end{cases}$$

$$V_{2,n}^{2,j}(x) = \begin{cases} \sqrt{2^{n-2}} V_{2,2}^2[2^{n-2}(x - \frac{j-1}{2^{n-2}})], & x \in (\frac{j-1}{2^{n-2}}, \frac{j}{2^{n-2}}), \\ 0, & \text{others}, \end{cases}$$

$$V_{2,n}^{3,j}(x) = \begin{cases} \sqrt{2^{n-2}} V_{2,2}^3[2^{n-2}(x - \frac{j-1}{2^{n-2}})], & x \in (\frac{j-1}{2^{n-2}}, \frac{j}{2^{n-2}}), \\ 0, & \text{others}, \end{cases}$$

where $j = 1, 2, \cdots, 2^{n-2}$, and $n = 3, 4, \cdots$.

For $k = 3$, the V-system is

$$V_{3,1}^1(x) = 1, \ x \in [0, 1],$$
$$V_{3,1}^2(x) = \sqrt{3}(1 - 2x), \ x \in [0, 1],$$
$$V_{3,1}^3(x) = \sqrt{5}(6x^2 - 6x + 1), \ x \in [0, 1],$$
$$V_{3,1}^4(x) = \sqrt{7}(-20x^3 + 30x^2 - 12x + 1), \ x \in [0, 1],$$

$$V_{3,2}^1(x) = \begin{cases} \sqrt{7}(-64x^3 + 66x^2 - 18x + 1), & x \in [0, \frac{1}{2}), \\ \sqrt{7}[-64(1-x)^3 + 66(1-x)^2 \\ \qquad - 18(1-x) + 1], & x \in [\frac{1}{2}, 1), \end{cases}$$

$$V_{3,2}^2(x) = \begin{cases} \sqrt{5}(-140x^3 + 114x^2 - 24x + 1), & x \in [0, \frac{1}{2}), \\ \sqrt{5}[140(1-x)^3 - 114(1-x)^2 \\ \qquad + 24(1-x) - 1], & x \in [\frac{1}{2}, 1), \end{cases}$$

$$V_{3,2}^3(x) = \begin{cases} \sqrt{3}(-224x^3+156x^2 - 28x + 1), & x \in [0, \frac{1}{2}), \\ \sqrt{3}[-224(1-x)^3 + 156(1-x)^2 \\ \qquad -28(1-x) + 1], & x \in [\frac{1}{2}, 1), \end{cases}$$

$$V_{3,2}^4(x) = \begin{cases} -280x^3 + 180x^2 - 30x + 1, & x \in [0, \frac{1}{2}), \\ 280(1-x)^3 - 180(1-x)^2 + \\ \qquad 30(1-x) - 1, & x \in [\frac{1}{2}, 1). \end{cases}$$

The general terms of the V-system of degree 3 are given by

$$V_{3,n}^{1,j}(x) = \begin{cases} \sqrt{2^{n-2}} V_{3,2}^1[2^{n-2}(x - \frac{j-1}{2^{n-2}})], & x \in (\frac{j-1}{2^{n-2}}, \frac{j}{2^{n-2}}), \\ 0, & \text{others}. \end{cases}$$

$$V_{3,n}^{2,j}(x) = \begin{cases} \sqrt{2^{n-2}} V_{3,2}^2[2^{n-2}(x - \frac{j-1}{2^{n-2}})], & x \in (\frac{j-1}{2^{n-2}}, \frac{j}{2^{n-2}}), \\ 0, & \text{others}. \end{cases}$$

$$V_{3,n}^{3,j}(x) = \begin{cases} \sqrt{2^{n-2}} V_{3,2}^3[2^{n-2}(x - \frac{j-1}{2^{n-2}})], & x \in (\frac{j-1}{2^{n-2}}, \frac{j}{2^{n-2}}), \\ 0, & \text{others}. \end{cases}$$

$$V_{3,n}^{4,j}(x) = \begin{cases} \sqrt{2^{n-2}} V_{3,2}^4[2^{n-2}(x - \frac{j-1}{2^{n-2}})], & x \in (\frac{j-1}{2^{n-2}}, \frac{j}{2^{n-2}}), \\ 0, & \text{others}. \end{cases}$$

where $j = 1, 2, \cdots, 2^{n-2}$, and $n = 3, 4, \cdots$.

REFERENCES

[1] G. Carneiro, A. B. Chan, P. J. Moreno, and N. Vasconcelos, "Supervised learning of semantic classes for image annotation and retrieval," *IEEE Trans. Pattern Anal. Mach. Intell.*, vol. 29, no. 3, pp. 394–410, Mar. 2007.
[2] S. Wang, J. Zhang, T. X. Han, and Z. Miao, "Sketch-based image retrieval through hypothesis-driven object boundary selection with HLR descriptor," *IEEE Trans. Multimedia*, vol. 17, no. 7, pp. 1045–1057, Jul. 2015.
[3] S. B. K. Aires, C. O. A. de Freitas, and L. S. Oliveira, "SIFT applied to perceptual zoning for trademark retrieval," in *Proc. IEEE Int. Conf. Syst., Man, Cybern.*, Oct. 2015, pp. 2401–2406.
[4] S. S. Husain and M. Bober, "Improving large-scale image retrieval through robust aggregation of local descriptors," *IEEE Trans. Pattern Anal. Mach. Intell.*, vol. 39, no. 9, pp. 1783–1796, Sep. 2017.
[5] C. Aker, O. Tursun, and S. Kalkan, "Analyzing deep features for trademark retrieval," in *Proc. 25th Signal Process. Commun. Appl. Conf. (SIU)*, May 2017, pp. 1–4.
[6] T. Lan, X. Feng, Z. Xia, S. Pan, and J. Peng, "Similar trademark image retrieval integrating LBP and convolutional neural network," in *Proc. Int. Conf. Image Graph.* Shanghai, China: Springer, Dec. 2017, pp. 231–242.
[7] O. Tursun, C. Aker, and S. Kalkan. (2017). "A large-scale dataset and benchmark for similar trademark retrieval." [Online]. Available: https://arxiv.org/abs/1701.05766
[8] O. Tursun, S. Denman, S. Sivipalan, S. Sridharan, C. Fookes, and S. Mau. (2018). "Component-based attention for large-scale trademark retrieval." [Online]. Available: https://arxiv.org/abs/1811.02746
[9] Z. Chen and X. Wang, "Trademark image retrieval system based on SIFT algorithm," in *Proc. IEEE/ACIS 17th Int. Conf. Comput. Inf. Sci. (ICIS)*, Jun. 2018, pp. 740–743.
[10] J. Wang *et al.*, "MindCamera: Interactive sketch-based image retrieval and synthesis," *IEEE Access*, vol. 6, pp. 3765–3773, 2018.
[11] N. Farajzadeh, "Exemplar-based logo and trademark recognition," *Mach. Vis. Appl.*, vol. 26, no. 6, pp. 791–805, Aug. 2015.
[12] P. Tripathi and A. K. Indoria, "Extraction and recognition of multi-oriented text from trademark images," in *Proc. Int. Conf. Cogn. Comput. Inf. Process. (CCIP)*, Mar. 2015, pp. 1–5.
[13] A. Wang, J. Lu, J. Cai, T.-J. Cham, and G. Wang, "Large-margin multi-modal deep learning for RGB-D object recognition," *IEEE Trans. Multimedia*, vol. 17, no. 11, pp. 1887–1898, Nov. 2015.
[14] C. Huang, Z. He, G. Cao, and W. Cao, "Task-driven progressive part localization for fine-grained object recognition," *IEEE Trans. Multimedia*, vol. 18, no. 12, pp. 2372–2383, Dec. 2016.

[15] K. Wang, C. Gou, N. Zheng, J. M. Rehg, and F.-Y. Wang, "Parallel vision for perception and understanding of complex scenes: Methods, framework, and perspectives," *Artif. Intell. Rev.*, vol. 48, no. 3, pp. 299–329, Oct. 2017.
[16] A. Caglayan and A. B. Can, "Volumetric object recognition using 3-D CNNs on depth data," *IEEE Access*, vol. 6, pp. 20058–20066, 2018.
[17] L. Pinjarkar, M. Sharma, and S. Selot, "Deep CNN combined with relevance feedback for trademark image retrieval," *J. Intell. Syst.*, to be published. doi: 10.1515/jisys-2018-0083.
[18] J. Chen *et al.*, "Polar transformation on image features for orientation-invariant representations," *IEEE Trans. Multimedia*, vol. 21, no. 2, pp. 300–313, Feb. 2019.
[19] S. Berretti, A. D. Bimbo, and P. Pala, "Retrieval by shape similarity with perceptual distance and effective indexing," *IEEE Trans. Multimedia*, vol. 2, no. 4, pp. 225–239, Dec. 2000.
[20] B. Horowitz, "Find images by color, shape, and texture [New Products]," *IEEE Multimedia Mag.*, vol. 2, no. 3, p. 78, 1995.
[21] A. W. Smeulders, M. Worring, S. Santini, A. Gupta, and R. Jain, "Content-based image retrieval at the end of the early years," *IEEE Trans. Pattern Anal. Mach. Intell.*, vol. 22, no. 12, pp. 1349–1380, Dec. 2000.
[22] Y. Rui, T. S. Huang, M. Ortega, and S. Mehrotra, "Relevance feedback: A power tool for interactive content-based image retrieval," *IEEE Trans. Circuits Syst. video Technol.*, vol. 8, no. 5, pp. 644–655, Sep. 1998.
[23] B. M. Mehtre, M. S. Kankanhalli, and W. F. Lee, "Shape measures for content based image retrieval: A comparison," *Inf. Process. Manage.*, vol. 33, no. 3, pp. 319–337, May 1997.
[24] R. C. Veltkamp and M. Tanase, "Content-based image retrieval systems: A survey," Dept. Comput. Sci., Utrecht Univ., Utrecht, The Netherlands, Tech. Rep. UU-CS-2000-34, 2000.
[25] S.-C. Chen, S. H. Rubin, M.-L. Shyu, and C. Zhang, "A dynamic user concept pattern learning framework for content-based image retrieval," *IEEE Trans. Syst., Man, Cybern. C, Appl. Rev.*, vol. 36, no. 6, pp. 772–783, Nov. 2006.
[26] R. Rahmani, S. A. Goldman, H. Zhang, S. R. Cholleti, and J. E. Fritts, "Localized content based image retrieval," *IEEE Trans. Pattern Anal. Mach. Intell.*, vol. 30, no. 11, pp. 1902–1912, Nov. 2008.
[27] A. Raza, H. Dawood, H. Dawood, S. Shabbir, R. Mehboob, and A. Banjar, "Correlated primary visual texton histogram features for content base image retrieval," *IEEE Access*, vol. 6, pp. 46595–46616, 2018.
[28] Y.-Y. Feng and D.-X. Qi, "A sequence of piecewise orthogonal polynomials," *SIAM J. Math. Anal.*, vol. 15, no. 4, pp. 834–844, Jul. 1984.
[29] R. Song, H. Ma, T. Wang, and D. Qi, "The complete orthogonal V-system and its applications," *Commun. Pure Appl. Anal.*, vol. 6, no. 3, pp. 853–871, Jul. 2007.
[30] R. Song, X. Wang, M. Ou, and J. Li, "The structure of V-system over triangulated domains," in *Proc. Int. Conf. Geometric Modeling Process.* Hangzhou, China: Springer, Apr. 2008, pp. 563–569.
[31] R. Song, Y. Liang, X. Wang, and D. Qi, "Elimination of Gibbs phenomenon in Computational Information based on the V-system," in *Proc. 2nd Int. Conf. Pervasive Comput. Appl.*, Jul. 2007, pp. 337–341.
[32] R. Song and M. Ou, "The application of V-system in the digital image transform," in *Proc. Int. Conf. Inf. Automat.*, Jun. 2008, pp. 296–301.
[33] R. Song, Z. Zhao, Y. Li, Q. Zhang, and C. Xi, "The method of shape recognition based on v-system," in *Proc. Int. Conf. Frontier Comput. Sci. Technol.*, Aug. 2010, pp. 321–326.
[34] Z. Li, X. Men, Y. Liu, and H. Li, "3d model retrieval based on v system rotation invariant moments," in *Proc. 3rd Int. Conf. Natural Comput. (ICNC)*, vol. 2, Aug. 2007, pp. 565–569.
[35] H. Wilbraham, "On a certain periodic function," *Camb. Dublin Math. J.*, vol. 3, no. 3, pp. 198–201, 1848.
[36] E. Hewitt and R. E. Hewitt, "The Gibbs-Wilbraham phenomenon: An episode in Fourier analysis," *Arch. Hist. Exact Sci.*, vol. 21, no. 2, pp. 129–160, Jun. 1979.
[37] J. W. Gibbs, "Fourier's series," *Nature*, vol. 59, no. 1522, p. 200, Dec. 1898. doi: 10.1038/059606a0.
[38] J. W. Gibbs, "Fourier's series," *Nature*, vol. 59, no. 1539, p. 606, 1899.
[39] S. Jeannin and M. Bober, *Description of Core Experiments for MPEG-7 Motion/Shape*, document MPEG-7, ISO/IEC/JTC1/SC29/WG11/MPEG99 N, vol. 2690, 1999.
[40] T. B. Sebastian, P. N. Klein, and B. B. Kimia, "Recognition of shapes by editing their shock graphs," *IEEE Trans. Pattern Anal. Mach. Intell.*, vol. 26, no. 5, pp. 550–571, May 2004.

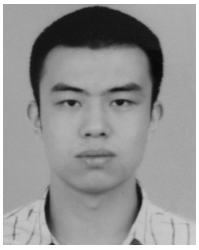

BEN YE received the B.S. degree from Beijing Normal University, Zhuhai, China, in 2013, and the master's degree from the Faculty of Information Technology, Macau University of Science and Technology, Macau, China, in 2015, where he is currently pursuing the Ph.D. degree with the Faculty of Information Technology.

His research interests include image processing, computer graphics, high-resolution image stitching, and remote sensing data processing and analysis.

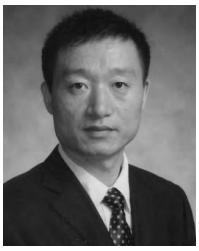

ZHANCHUAN CAI (M'16–SM'19) received the Ph.D. degree from Sun Yat-sen University, Guangzhou, China, in 2007.

From 2007 to 2008, he was a Visiting Scholar with the University of Nevada, Las Vegas, NV, USA. He is currently a Professor with the Faculty of Information Technology, Macau University of Science and Technology, Macau, China, where he is also with the State Key Laboratory of Lunar and Planetary Science. His research interests include image processing, computer graphics, and lunar data processing and analysis.

Prof. Cai is a member of the ACM, the Chang'e-3 Scientific Data Research and Application Core Team, and the Asia Graphics Association. He is also a Senior Member of the CCF. He was a recipient of the Third prize of the Macau Science and Technology Award-Natural Science Award, in 2012, the BOC Excellent Research Award from the Macau University of Science and Technology, in 2016, and the Third Prize of the Macau Science and Technology Award-Technological Invention Award, in 2018.

TING LAN received the M.S. degree from the University of Macau, Macau, China, in 2014, and the Ph.D. degree from the Faculty Information Technology, Macau University of Science and Technology, Macau, China, in 2019.

His research interests include image processing, computer graphics, and remote sensing data processing.

Dr. Lan was a recipient of the First Prize at the 14th China Postgraduate Mathematical Contest in Modeling, China Academic Degrees and Graduate Education Development Center and China Graduate Mathematical Contest in Modeling Committee, in 2017, and the Third Prize of the Macau Science and Technology Award-Technological Invention Award, in 2018.

YOUQING XIAO received the M.S. degree in computer software and theory from Sun Yat-sen University, in 2005. He is currently pursuing the Ph.D. degree with the Faculty of Information Technology, Macau University of Science and Technology. He was with The Hong Kong Polytechnic University as a Research Assistant, from 2007 to 2008. He was a Lecturer with the Beijing Institute of Technology, Zhuhai.

His research interests include image processing and computer graphics.